DYNAMIC COUPLING OF UNDERACTUATED MANIPULATORS

Marcel Bergerman Christopher Lee Yangsheng Xu

CMU-RI-TR-94-25

The Robotics Institute
Carnegie Mellon University
Pittsburgh, Pennsylvania 15213

August, 1994

This research is partially sponsored by the Brazilian National Council for Research and Development (CNPq). The views and conclusions contained in this document are those of the authors and should not be interpreted as representing the official policies or endorsements, either expressed or implied, of CNPq or Carnegie Mellon University.

Table of Contents

List of Figures

List of Tables

Abstract

In recent years, researchers have been dedicated to the study of underactuated manipulators which have more joints than control actuators. In previous works, one always assumes that there is enough dynamic coupling between the active and the passive joints of the manipulator, for it to be possible to control the position of the passive joints via the dynamic coupling. In this work, the authors aim to develop an index to measure the dynamic coupling, so as to address when control of the underactuated system is possible, and how the motion and robot configuration can be designed. We discuss extensively the nature of the dynamic coupling and of the proposed coupling index, and their applications in the analysis and design of underactuated systems, and in control and planning of robot motion configuration.

1 Introduction

In recent years, researchers have been turning their attention to so called underactuated systems, where the term *underactuated* refers to the fact that the system has more joints than control actuators. Some examples of underactuated systems are robot manipulators with failed actuators; free-floating space robots, where the base can be considered as a virtual passive linkage in inertia space; legged robots with passive joints; hyper-redundant (snake-like) robots with passive joints, etc.

From the examples above, it is possible to justify the importance of the study of underactuated systems. For example, if some actuators of a conventional manipulator fail, the loss of one or more degrees of freedom may compromise an entire operation. In free-floating space systems, the base (satellite) can be considered as a 6-DOF device without positioning actuators. Finally, manipulators with passive joints and hyper-redundant robots with few actuators are important from the viewpoint of energy saving, lightweight design and compactness.

Most of the results available in the literature for fully-actuated systems are difficult to apply to these new ones, because of the complications that appear in their dynamic formulation. Manipulators with passive joints present nonholonomic constraints, and the conditions for integrability of these constraints are too stringent [9]. In general, the control system must cope with these constraints and hopefully take advantage of them to guarantee stability and performance requirements. Furthermore, as opposed to conventional manipulators, in this problem there is a guarantee that no smooth control law can achieve stability of the system to an equilibrium point [7], [9]. Thus, one is left with the choice of procuring a discontinuous control law to reach a desired equilibrium position, or being content with controlling the system to an equilibrium manifold.

Some recent works present a control strategy to deal with the joint and Cartesian control problem of underactuated manipulators. Arai and Tachi [1] presented a method which required brakes to be installed on each passive joints. The basic idea was to use the dynamic coupling between the active and the passive joints, in order to drive the passive joints to a desired set-point. Later, Bergerman and Xu [2] enhanced this method to deal with parameter uncertainty and provide the system with a greater deal of robustness. This is specially important in these systems because the Jacobian mapping from Cartesian to joint space depends on the dynamic parameters, once again differently from conventional robots, where

the Jacobian depends solely on kinematic parameters. Parameter uncertainty can lead the system to a very poor or even unstable performance. Another interesting control strategy requiring the use of brakes was done by Papadopoulos and Dubowsky [10], this time for a space manipulator.

In every work mentioned above, the authors had to assume that “enough” coupling existed between the passive and the active joints, so that the controller could “transmit” the forces/torques to the passive joints in order to drive them. However, no attempts were made to quantify this coupling, or to identify the cases when it is too small as to be practically unfeasible to control the passive joints. To give the reader an introductory feeling of the importance of the dynamic coupling in underactuated mechanisms, consider a Cartesian 3-DOF manipulator, where the joint axes are mutually perpendicular. It can be verified that the inertia matrix for this manipulator is diagonal and constant, corresponding to the physical fact that there is no coupling at all between the joints. No matter how much one joint travels, the other ones are unaffected. Consequently, the absence of coupling does not allow this mechanism to be controlled at all if passive joints are present.

In this work, the authors aim to provide a measure of the dynamic coupling present in underactuated systems. This measure is useful not only for the design of an underactuated manipulator, so as to maximize the coupling and hopefully minimize the energy necessary to perform control; it is also useful for such important issues as actuator placement and control strategies. In cases for which the number of actuators is greater than the number of passive joints, such a measure can also be used in connection with a redundant control scheme [8], in order to maintain the system as far as possible from the positions that yield low dynamic coupling.

2 Dynamic Coupling

As mentioned before, the nonholonomic constraints present in the dynamic equation of a manipulator with passive joints cannot be integrated in general. Even partial integrability of the acceleration relationships to velocity ones is not possible in most cases [9]. This restriction makes it impossible to obtain a direct relationship between the angles of the passive joints and that of the active ones. Thus, it is necessary to work with the dynamic equations in their original form, and to try to derive acceleration relationships to quantify the dynamic coupling.

In order to derive the measure of dynamic coupling between the accelerations of the passive and active joints of an underactuated manipulator, we must first present the dynamic equations governing the behavior of the system. Let n be the total number of joints, r the number of active joints, and $p = n - r$ the number of passive ones. By using either the Newton-Euler or the Lagrangian formulation [3], one can obtain the following set of differential equations relating the accelerations of the joints to the torques supplied by the actuators:

$$M(q)\,\ddot{q} + b(q, \dot{q}) = \tau \tag{1}$$

Here, the matrix M is the n x n inertia matrix of the manipulator, b is a vector containing all the centrifugal, Coriolis and gravitational torques, and τ is the vector of torques applied at the active joints. Note that τ has always p components equal to zero, corresponding to the absence of actuators at the passive joints.

Equation (1) is not useful in its current form, for it does not reveal the relationship between the active and the passive joints' velocities and accelerations. If we partition the joint vector q as:

$$q = \begin{bmatrix} q_a & q_p \end{bmatrix}^T \tag{2}$$

where q_a correspond to the active joint angles and q_p to the passive ones, the following partition can be performed on the dynamic equation:

$$\begin{matrix} r \\ p \end{matrix} \begin{bmatrix} M_{aa} & M_{ap} \\ M_{pa} & M_{pp} \end{bmatrix} \begin{bmatrix} \ddot{q}_a \\ \ddot{q}_p \end{bmatrix} + \begin{bmatrix} b_a \\ b_p \end{bmatrix} = \begin{bmatrix} \tau_a \\ 0 \end{bmatrix} \tag{3}$$
$$\begin{matrix} & r & p \end{matrix}$$

It must be noted that M as defined in (3) *is not always equal* to the conventional inertia matrix of mechanical manipulators. Nonetheless, M still preserves important properties of the original inertia matrix, such as symmetry and positive-definiteness. To see this, note that the new inertia matrix is obtained from the original one after the swapping of rows and columns in an orderly fashion: if rows i and j are swapped, so must be columns i and j.

This swapping operation can be represented as a matrix product. In order to avoid confusion, let's denote by M_o the original manipulator's inertia matrix, and by M the one

representing the active and passive joints of the system, as in (3). The process of obtaining M via the swapping of rows and columns of M_o can be described mathematically as:

$$M = TM_oT \tag{4}$$

where T is a transformation matrix obtained from the identity matrix by the swapping of rows i and j (or columns i and j):

$$T = \begin{bmatrix} 1 & & & & & & \\ & 1 & & & & & \\ & & 0 & & 1 & & \leftarrow \text{row } i \\ & & & 1 & & & \\ & & 1 & & 0 & & \leftarrow \text{row } j \\ & & & & & 1 & \\ & & & & & & 1 \end{bmatrix} \tag{5}$$

Since T is obtained from the identity matrix via an elementary operation, it is invertible (actually, T is also an elementary matrix). Furthermore, it can be verified that it is equal to its inverse:

$$T = T^{-1} \tag{6}$$

This allows us to write:

$$M = TM_oT^{-1} \tag{7}$$

and to establish that M and M_o are *similar matrices*. Now it is a known fact that the spectrum of similar matrices are the same (for a proof, see [5], p. 152), and so we can conclude that the new inertia matrix of the manipulator, M, is positive definite.

Additionally, we can show that M is also symmetric. It is known that the original inertia matrix is symmetric, and that the transformation T is also symmetric. This allows us to write:

$$M^T = (TM_oT)^T = T^TM_o^TT^T = TM_oT = M \tag{8}$$

and to conclude on the symmetry of M.

The submatrices of M in (3) receive their indexes according to the variables they relate. For example, M_{pa} relates the (null) torques at the passive joints to the acceleration of the active ones. The same reasoning is true for the other three submatrices. From the second line of (3), we can write:

$$M_{pa}\ddot{q}_a + M_{pp}\ddot{q}_p + b_p = 0 \tag{9}$$

or, in the cases where M_{pp} is invertible:

$$\ddot{q}_p = -M_{pp}^{-1}M_{pa}\ddot{q}_a - M_{pp}^{-1}b_p \tag{10}$$

The second term on the right-hand side of (10) is a function only of q and $\dot{q}$, and as such is completely determined once measurements of these variables are available. Because we are focusing on the acceleration relationship between the active and the passive joints, we rewrite equation (10) as:

$$\begin{aligned} \ddot{\bar{q}}_p &= -M_{pp}^{-1}M_{pa}\ddot{q}_a \\ &\equiv M_c\ddot{q}_a \end{aligned} \tag{11}$$

where

$$\ddot{\bar{q}}_p = \ddot{q}_p + M_{pp}^{-1}b_p \tag{12}$$

The acceleration $\ddot{\bar{q}}_p$ can be viewed as a virtual acceleration of the passive joints, generated by the acceleration of the active ones, and by the nonlinear torques due to velocity effects. Given a desired acceleration of the passive joints, $\ddot{q}_{p,\,d}$, we can always determine at every sampling instant the desired acceleration for $\ddot{\bar{q}}_p$ as:

$$\ddot{\bar{q}}_{p,\,d}(t) = \ddot{q}_{p,\,d}(t) + M_{pp}^{-1}b_p(t-\Delta t) \tag{13}$$

The control problem reduces to finding the $\ddot{q}_a$ in (11) that guarantees that:

$$\ddot{\bar{q}}_p = \ddot{\bar{q}}_{p,\,d} \tag{14}$$

Equation (11) is important in the understanding of how an underactuated system works. Torques can only be applied at those joints which contain an actuator, or the active joints. These torques produce the accelerations $\ddot{q}_a$, which indirectly produce the accelerations $\ddot{q}_p$

at the passive joints. The passive joints' accelerations can only be controlled if the p x r matrix M_c possesses a structure that allows the actuators torques to be transmitted reasonably "well" (in a sense to be defined later) to the passive joints. Thus, the study of this matrix is of fundamental importance for the design and control of underactuated manipulators.

To begin the analysis, note that matrix M_c is a function only of the robot's configuration q, and thus is completely determined based on the readings of the encoders in all joints. It does not depend on $\ddot{q}_a$ or $\ddot{q}_p$. Thus, equation (11) can be regarded as a linear system of p equations $Ax = b$, underconstrained for $r > p$ and overconstrained for $r < p$.

One result that can be immediately derived from the structure of (11) is:

Proposition 1 If row i, $1 \le i \le p$, in matrix M_c contains only zeros, then the i-th passive joint cannot be controlled via the dynamic coupling with the active joints.

This propositions follows from the fact that, if M_c has a line of zeros, then the i-th line in equation (10) reduces to:

$$\ddot{q}_{p_i} = \left(-M_{pp}^{-1} b_p \right)_i \tag{15}$$

This equality indicates that the acceleration of the i-th passive joint is not a function of any of the active joints' accelerations, and thus cannot be controlled directly.

Example 1 Consider a simple two-link manipulator as shown in Figure 1. Joint 1 rotates around the Z axis, while joint 2 rotates around an axis perpendicular to the first joint axis. The inertia matrix M for this system is:

$$M = \begin{bmatrix} m_2 l_{c_2}^2 \sin(\theta_2)^2 + I_1 + I_2 & 0 \\ 0 & m_2 l_{c_2}^2 + I_2 \end{bmatrix} \tag{16}$$

where m_2 is the mass of link 2, I_i are the inertias of links i = 1, 2, and l_{c_2} is the distance between joint 2 and the center of gravity of link 2. Two cases can be considered here: either joint 1 is active and joint 2 is passive, or vice-versa. For the first case, we have:

$$M_{pa} = 0, \qquad M_{pp} = m_2 l_{c_2}^2 + I_2 \tag{17}$$

and therefore:

$$M_c = 0 \tag{18}$$

Equation (17) indicates that it is not possible to control $\ddot{q}_2$ via its coupling with $\ddot{q}_1$. Thus, this underactuated system would not be useful for practical purposes. In the case for which joint 1 is passive, the result is the same:

$$M_{pa} = 0, \qquad M_{pp} = m_2 l_{c_2}^2 \sin(\theta_2)^2 + I_1 + I_2 \tag{19}$$

and therefore:

$$M_c = 0 \tag{20}$$

We can conclude that this mechanism's structure does not allow its passive joint to be controlled through the coupling with the active one, whether the active joint is joint 1 or 2. Note that the above statement *does not imply that* the joints do not have any coupling at all. In fact, the second term in the right-hand side of (10) is generally non-zero, and so the passive joint may be disturbed for a given motion of the active one. However, the acceleration of the passive joint due to the coupling is non-controllable. ■

Example 2 Consider now the 2-link planar manipulator shown in Figure 2. For this system, we have:

$$M = \begin{bmatrix} m_1 l_{c_1}^2 + m_2\left[l_1^2 + l_{c_2}^2 + 2 l_1 l_{c_2}\cos(\theta_2)\right] + I_1 + I_2 & m_2\left[l_{c_2}^2 + l_1 l_{c_2}\cos(\theta_2)\right] + I_2 \\ m_2\left[l_{c_2}^2 + l_1 l_{c_2}\cos(\theta_2)\right] + I_2 & m_2 l_{c_2}^2 + I_2 \end{bmatrix} \tag{21}$$

Considering joint 1 active, and joint 2 passive, we have:

$$M_{pa} = m_2\left[l_{c_2}^2 + l_1 l_{c_2}\cos(\theta_2)\right] + I_2, \qquad M_{pp} = m_2 l_{c_2}^2 + I_2 \tag{22}$$

$$M_c = -\left[1 + \frac{m_2 l_1 l_{c_2}\cos(\theta_2)}{m_2 l_{c_2}^2 + I_2}\right] \tag{23}$$

Note that for this mechanism the structure does not prevent torque from being transmitted from the active to the passive joint, as it was the case in example 1. A numerical characterization of this transmission will be given in section 3. ■

3 Dynamic Coupling Measure

As long as the sub-matrix M_{pp} is invertible, we can study the relationship between the accelerations of the passive and active joints:

$$\ddot{q}_p = M_c \ddot{q}_a$$

According to our definition, M_c is a p x r matrix. We must study the various possibilities that can arise depending on whether there are more active or more passive joints in the mechanism. The first consideration that can be made regards the rank of matrix M_c. It is known that this rank obeys:

$$\text{rank}\,(M_c) \leq \min\,(p, r) \tag{24}$$

This fact will be used in the sequence.

• Case 1: $r < p$

Although this may not be common, it may happen that the number of actuators is smaller than the number of passive joints (e.g., when two actuators of a 3-DOF arm fail). In this case, M_c has maximum rank r, and equation (11) has *at most* one solution. However, this solution (if it exists) is not interesting in practice, because the accelerations of $p - r$ passive joints will depend linearly on the accelerations of the other r passive joints. In other words, r passive joints can be controlled at every instant, while the other $p - r$ of them cannot. We can conclude that it is necessary to have *at least p* actuators in the underactuated mechanism to be possible to control all p passive joints independently. Note that this result was already established by Arai and Tachi [1]; however in their work, the authors reached this conclusion only after a study of the linearized dynamic equations of the system.

Although it is not possible to control all p passive joints when $r < p$, we can resort to the least-square solution in order to find the $\ddot{q}_a$ that generates the "best" $\ddot{q}_p$ (in a least-squares sense) for all (or some) passive joints.

• Case 2: $r = p$

In this case we can obtain at most one solution, which exists if the r x r matrix M_c is invertible (or, in other words, if both matrices M_{pp} and M_{pa} are invertible). A case-by-case pre-analysis of M_c can show whether it will be possible to control $\ddot{q}_p$ using the actuators at the active joints.

• Case 3: $r > p$

This is probably the most common case, and certainly the most interesting one. Here, we can obtain *at least* one solution for the problem of finding the $\ddot{q}_a$ that will generate the desired $\ddot{q}_p$, provided the rank of matrix M_c is at least equal to p. In the general case, infinite solutions can be found. One can choose among these solutions the one that provides the minimum norm of $\ddot{q}_a$, so as to save energy, or effectively make use of this redundancy to accomplish tasks such as obstacle avoidance, actuability maximization [6], etc.

In any of the cases above, it is useful to define a measure of the dynamic coupling at any given instant. For example, when dealing with case 3, we can try to maximize the coupling via the use of the redundancy present in the system. Following [6], [11], it is natural to think of the singular values of M_c, which quantify its "degree of invertibility" and thus its capacity to "transmit" the torque from the active to the passive joints. Based on this, let $\sigma_1 \geq \sigma_2 \geq \ldots \geq \sigma_c$ be the $c = \min(p, r)$ singular values of M_c. Possible measures of the dynamic coupling are:

$$\rho_c = \begin{cases} \sqrt{\det\left(M_c^T M_c\right)} & \text{if} \quad r < p \\ \left|\det\left(M_c\right)\right| & \text{if} \quad r = p \\ \sqrt{\det\left(M_c M_c^T\right)} & \text{if} \quad r > p \end{cases} \tag{25}$$

In any case,

$$\rho_c = \prod_{i=1}^{c} \sigma_i \tag{26}$$

We call ρ_c as above the *coupling index* of the underactuated manipulator. As will be shown in the sequence, the coupling index can be used as a design tool for actuator placement,

desirable robot configuration, or as a quantity to be used on the real-time control of the manipulator.

Example 3 Let's retake example 2, and apply the coupling index concept to it. We saw that:

$$M_c = -\left[1 + \frac{m_2 l_1 l_{c_2} \cos(\theta_2)}{m_2 l_{c_2}^2 + I_2}\right] \tag{27}$$

Since M_c is a scalar, we have:

$$\rho_c = \left|1 + \frac{m_2 l_1 l_{c_2} \cos(\theta_2)}{m_2 l_{c_2}^2 + I_2}\right| \tag{28}$$

Let's adopt the following parameters for the quantities above: $m_2 = 1\text{Kg}$, $l_1 = 0.3\text{m}$, $l_{c_2} = 0.15\text{m}$, $I_2 = 0.1\text{Kg}\cdot\text{m}^2$. Then:

$$\rho_c = \left|1 + 0.37\cos\theta_2\right| \tag{29}$$

We see that, for this manipulator, the matrix M_c is *always* invertible, and thus control of the passive joint via the dynamic coupling is always possible. Based on the present study, one can now pre-analyze the system in order to determine whether or not control is possible, before making any attempt to control it. ■

4 Manipulator Design

The coupling index derived previously can be used effectively on the design of the underactuated system as a mathematical tool that determines the optimal actuator placement of an underactuated manipulator. In the following we will use a series of examples to illustrate its importance.

Example 4 If we consider the same manipulator as in example 3, but now with joint 1 as the passive joint, we have the following results[1]:

1. The bars over the matrices were added so as to avoid confusion with the previous example.

$$\begin{aligned} \overline{M}_{pa} &= m_2\left[l_{c_2}^2 + l_1 l_{c_2}\cos(\theta_2)\right] + I_2 \\ \overline{M}_{pp} &= m_1 l_{c_1}^2 + m_2\left[l_1^2 + l_{c_2}^2 + 2l_1 l_{c_2}\cos(\theta_2)\right] + I_1 + I_2 \end{aligned} \tag{30}$$

Therefore:

$$\overline{M}_c = -\frac{m_2\left[l_{c_2}^2 + l_1 l_{c_2}\cos(\theta_2)\right] + I_2}{m_1 l_{c_1}^2 + m_2\left[l_1^2 + l_{c_2}^2 + 2l_1 l_{c_2}\cos(\theta_2)\right] + I_1 + I_2} \tag{31}$$

Substituting the values $m_1 = 2\text{Kg}$, $I_1 = 0.2\text{Kg}\cdot\text{m}^2$ in addition to the ones previously adopted, we have:

$$\begin{aligned} \overline{M}_c &= -\frac{0.1225 + 0.045\cos\theta_2}{0.4575 + 0.090\cos\theta_2} \\ \bar{\rho}_c &= \left|\frac{0.1225 + 0.045\cos\theta_2}{0.4575 + 0.090\cos\theta_2}\right| \end{aligned} \tag{32}$$

Figure 3 shows how ρ_c and $\bar{\rho}_c$ vary as a function of θ_2. From this figure, we can infer that it is “easier” for joint 1 to drive joint 2 than vice-versa, because of the greater coupling available in the average for the lower-actuated manipulator than that for the upper-actuated one. Thus, the coupling index indicates that, for the purpose of maximizing the dynamic coupling, joint 1 should be the active one, and joint 2 should be passive. ■

Note how this approach differs from the one studied by Lee and Xu [6], where the authors defined the *actuability index* of underactuated manipulators. The actuability index measures the arbitrariness of the actuator’s ability to cause acceleration at the end-effector. Thus, *it relates torques in the active joints and accelerations at the end-effector in Cartesian space*, while the coupling index defined in this work *relates accelerations of the active joints to accelerations of the passive ones.* The conclusions derived in [6] and the ones here should not be compared, for the indexes operate in different manners. To be more specific, the coupling index indicates how much acceleration is possible to be obtained at the passive joints given limited accelerations at the active joints. There is no attempt to quantify the accelerations possible to be obtained at the end-effector. The actuability index indicates how much acceleration can be obtained at the end-effector given limited torques at the active joints. It does not attempt to quantify the accelerations at the passive joints.

In order to better provide the reader with an understanding of the difference between these two measures, we will briefly present the relationship of the acceleration of the end-effector to the torque at the active joint of the manipulator in example 4, for both upper- and lower-actuated cases. In the sequence, the subscripts *u* and *l* will be used to denote variables when the manipulator is, respectively, upper-actuated or lower-actuated.

The accelerations of the end-effector in *x* and *y* directions can be easily found to be:

$$\begin{aligned} \ddot{x} &= -\left[(l_1 c_1 + l_2 c_{12})\,\dot{\theta}_1^2 + 2 l_2 c_{12} \dot{\theta}_1 \dot{\theta}_2 + l_2 c_{12} \dot{\theta}_2^2 + (l_1 s_1 + l_2 s_{12})\,\ddot{\theta}_1 + l_2 s_{12} \ddot{\theta}_2 \right] \\ \ddot{y} &= -\left[(l_1 s_1 + l_2 s_{12})\,\dot{\theta}_1^2 + 2 l_2 s_{12} \dot{\theta}_1 \dot{\theta}_2 + l_2 s_{12} \dot{\theta}_2^2 - (l_1 c_1 + l_2 c_{12})\,\ddot{\theta}_1 - l_2 c_{12} \ddot{\theta}_2 \right] \end{aligned} \tag{33}$$

As before, we can consider the following virtual Cartesian accelerations, generated by the accelerations at the joints and the nonlinear effects:

$$\begin{aligned} \ddot{x} &= -\left[(l_1 s_1 + l_2 s_{12})\,\ddot{\theta}_1 + l_2 s_{12} \ddot{\theta}_2 \right] \\ \ddot{y} &= \left[(l_1 c_1 + l_2 c_{12})\,\ddot{\theta}_1 + l_2 c_{12} \ddot{\theta}_2 \right] \end{aligned} \tag{34}$$

Ignoring the nonlinear effects provenient from centrifugal, Coriolis and gravitational torques, from (1) we can write for the upper-actuated mechanism:

$$\begin{aligned} M_{2,1}\ddot{\theta}_1 + M_{2,2}\ddot{\theta}_2 &= 0 \quad \Rightarrow \quad \ddot{\theta}_2 = -(M_{2,1}/M_{2,2})\,\ddot{\theta}_1 \\ M_{1,1}\ddot{\theta}_1 + M_{1,2}\ddot{\theta}_2 &= \tau_u \quad \Rightarrow \quad \ddot{\theta}_1 = (M_{2,2}/\det(M))\,\tau \end{aligned} \tag{35}$$

where $M_{i,j}$ denotes the (*i*,*j*) element of the original inertia matrix. Substituting (35) into (34) we get:

$$\begin{aligned} \ddot{x}_u &= -\left[l_1 s_1 + l_2 s_{12} \left(1 - \frac{M_{2,1}}{M_{2,2}} \right) \right] \frac{M_{2,2}}{\det(M)} \tau_u \\ \ddot{y}_u &= \left[l_1 c_1 + l_2 c_{12} \left(1 - \frac{M_{2,1}}{M_{2,2}} \right) \right] \frac{M_{2,2}}{\det(M)} \tau_u \end{aligned} \tag{36}$$

For the lower-actuated manipulator, the results are:

$$\begin{aligned} M_{1,1}\ddot{\theta}_1 + M_{1,2}\ddot{\theta}_2 &= 0 \quad \Rightarrow \quad \ddot{\theta}_1 = -(M_{1,2}/M_{1,1})\,\ddot{\theta}_2 \\ M_{2,1}\ddot{\theta}_1 + M_{2,2}\ddot{\theta}_2 &= \tau_l \quad \Rightarrow \quad \ddot{\theta}_2 = (M_{1,1}/\det(M))\,\tau_l \end{aligned} \tag{37}$$

$$\begin{aligned} \ddot{x}_l &= -\left[-l_1 s_1\left(\frac{M_{1,2}}{M_{1,1}}\right) + l_2 s_{12}\left(1 - \frac{M_{1,2}}{M_{1,1}}\right)\right]\frac{M_{1,1}}{\det(M)}\tau_l \\ \ddot{y}_l &= \left[-l_1 c_1\left(\frac{M_{1,2}}{M_{1,1}}\right) + l_2 c_{12}\left(1 - \frac{M_{1,2}}{M_{1,1}}\right)\right]\frac{M_{1,1}}{\det(M)}\tau_l \end{aligned} \tag{38}$$

Figure 4 presents a comparison of the norm of the end-effector acceleration, $\|a\| = \sqrt{\ddot{x}^2 + \ddot{y}^2}$, which is a function of θ_2 only. The full line represents the upper-actuated mechanism, and the dashed line, the lower-actuated one. As we can see, the actuability of the upper-actuated mechanism is always greater than that of the lower-actuated one. This result contrasts with that represented by Figure 3, where we can see that the coupling index of the lower-actuated mechanism is always greater.

Finally, we borrow here an example from [6], to illustrate the comments above. For the same manipulator, the actuability ellipsoid is shown in Figures 5 and 6, respectively for the lower- and the upper-actuated mechanism. As we can see, the actuability index, which is proportional to the volume (length, in this case) of the actuability ellipsoid, is greater for upper-actuated mechanisms. We refer the reader to reference [6] for more detailed information on the actuability index.

Example 5 Let's consider now a "richer" example of a 3-DOF planar manipulator with rotary joints, as shown in Figure 7. The inertia matrix is given by:

$$M = \begin{bmatrix} M_{11} & M_{12} & M_{13} \\ M_{21} & M_{22} & M_{23} \\ M_{31} & M_{32} & M_{33} \end{bmatrix} \tag{39}$$

$$M_{11} = m_1 l_{c_1}^2 + m_2\left(l_1^2 + l_{c_2}^2 + 2 l_1 l_{c_2} c_2\right) + m_3\left(l_1^2 + l_2^2 + l_{c_3}^2 + 2 l_1 l_2 c_2 + 2 l_1 l_{c_3} c_{23} + 2 l_2 l_{c_3} c_3\right) + I_1 + I_2 + I_3$$

$$M_{12} = M_{21} = m_2\left(l_{c_2}^2 + l_1 l_{c_2} c_2\right) + m_3\left(l_2^2 + l_{c_3}^2 + l_1 l_2 c_2 + l_1 l_{c_3} c_{23} + 2 l_2 l_{c_3} c_3\right) + I_2 + I_3$$

$$M_{13} = M_{31} = m_3\left(l_{c_3}^2 + l_1 l_{c_3} c_{23} + l_2 l_{c_3} c_3\right) + I_3$$

$$M_{22} = m_2 l_{c_2}^2 + m_3\left(l_2^2 + l_{c_3}^2 + 2 l_2 l_{c_3} c_3\right) + I_2 + I_3$$

$$M_{23} = M_{32} = m_3\left(l_{c_3}^2 + l_2 l_{c_3} c_3\right) + I_3$$

$$M_{33} = m_3 l_{c_3}^2 + I_3$$

For simplicity, let's adopt the same parameters as in example 4, and adopt for link 3 the same mass, length and inertia of link 2. Then:

$$M = \begin{bmatrix} 0.7475 + 0.2700c_2 + 0.060c_{23} + 0.060c_3 & 0.3225 + 0.1350c_2 + 0.030c_{23} + 0.060c_3 & 0.1100 + 0.030c_{23} + 0.030c_3 \\ 0.3225 + 0.1350c_2 + 0.030c_{23} + 0.060c_3 & 0.3225 + 0.060c_3 & 0.1100 + 0.030c_3 \\ 0.1100 + 0.030c_{23} + 0.030c_3 & 0.1100 + 0.030c_3 & 0.1100 \end{bmatrix} \quad (40)$$

Let's assume $r = 2$, i.e., we have two actuators to be placed either on joints 1 and 2, 1 and 3 or 2 and 3. In either case, M_c is a 1 x 2 matrix, what indicates that *at least* one solution to the problem of finding $\ddot{q}_a$ for a desired $\ddot{q}_p$ exists, provided that both elements of M_c are not equal to zero at the same instant (one such possible solution was demonstrated in [2]). Let's compute the coupling index for each case[2]:

• Case 1: Joints 1 and 2 are active, joint 3 is passive

$$M_{c_1} = -\begin{bmatrix} 1 + 0.2727\,(c_{23} + c_3) & 1 + 0.2727c_3 \end{bmatrix} \quad (41)$$

• Case 2: Joints 1 and 3 are active, joint 2 is passive

$$M_{c_2} = -\begin{bmatrix} \dfrac{0.3225 + 0.1350c_2 + 0.030c_{23} + 0.060c_3}{0.3225 + 0.060c_3} & \dfrac{0.1100 + 0.030c_3}{0.3225 + 0.060c_3} \end{bmatrix} \quad (42)$$

• Case 3: Joints 2 and 3 are active, joint 1 is passive

$$M_{c_3} = -\begin{bmatrix} \dfrac{0.3225 + 0.1350c_2 + 0.030c_{23} + 0.060c_3}{0.7475 + 0.2700c_2 + 0.060c_{23} + 0.060c_3} & \dfrac{0.1100 + 0.030c_{23} + 0.030c_3}{0.7475 + 0.2700c_2 + 0.060c_{23} + 0.060c_3} \end{bmatrix} \quad (43)$$

Figures 8, 9 and 10 show the value of $\rho_{c_i}, i = 1, 2, 3$ as a function both θ_2 and θ_3. Figure 11 shows all these indexes combined. A careful consideration of these figures shows that, for most values of the joint angles, ρ_{c_1} is the greatest index of all three. This can be verified by the values in table 1. As we see, in none of the cases does ρ_{c_i} becomes zero (or "dangerously" close to zero). This indicates that at least one solution will always exist, no matter which joint is the passive one. Also, the choice of joint 3 as the passive joint increases the dynamic coupling, and enhances the control of the passive joint by the active ones. ■

2. Here, the indexes 1, 2 and 3 will be used to differentiate each case.

Table 1: Maximum, minimum, average and standard deviation values attained by ρ_{c_i}, $i = 1, 2, 3$.

i	$\max(\rho_{c_i})$	$\min(\rho_{c_i})$	$\text{avg}(\rho_{c_i})$	$\text{std}(\rho_{c_i})$
1	2.0021	0.8576	1.4211	0.3033
2	1.4774	0.6645	1.0607	0.2811
3	0.5104	0.3912	0.4556	0.0374

5 Sensitivity Analysis

As explained in [8], other indexes derived from the singular values of M_c can be useful. One of them is the *condition number* κ_c of M_c, defined as the ratio of the greatest to the smallest singular values. The condition number is very useful in the analysis of the sensitivity of equation (11). Even in the cases where ρ_c is "big" enough to guarantee the existence of dynamic coupling, the condition number can indicate that the relative errors between the acceleration of the active and the passive joints is also too big. In these cases, amplified noise can disturb the performance of the mechanism.

We will perform here a brief sensitivity analysis of (11), and see how this can influence the use of the coupling index. It is known that the norms of the accelerations in (11) obey:

$$\frac{1}{\sigma_1} \leq \frac{\|\ddot{q}_a\|}{\|\ddot{q}_p\|} \leq \frac{1}{\sigma_c} \tag{44}$$

If noise is present in the system and exhibits itself in the form of an error $\Delta\ddot{q}_p$ on $\ddot{q}_p$, then the corresponding error $\Delta\ddot{q}_a$ on $\ddot{q}_a$ obeys:

$$\frac{1}{\sigma_1} \leq \frac{\|\Delta\ddot{q}_a\|}{\|\Delta\ddot{q}_p\|} \leq \frac{1}{\sigma_c} \tag{45}$$

If the smallest singular value of M_c is too small, equation (45) shows that the acceleration of the active joints may include a magnified error due to the noise present in $\ddot{q}_p$.

Furthermore, from equations (44) and (45) we can conclude that the ratio of the relative errors obeys:

$$\frac{\sigma_c}{\sigma_1} \leq \frac{\left\|\Delta\ddot{q}_a\right\| / \left\|\ddot{q}_a\right\|}{\left\|\Delta\ddot{q}_p\right\| / \left\|\ddot{q}_p\right\|} \leq \frac{\sigma_1}{\sigma_c} \tag{46}$$

or, equivalently,

$$\frac{1}{\kappa_c} \leq \frac{\left\|\Delta\ddot{q}_a\right\| / \left\|\ddot{q}_a\right\|}{\left\|\Delta\ddot{q}_p\right\| / \left\|\ddot{q}_p\right\|} \leq \kappa_c \tag{47}$$

As we can see, the ratio of the relative errors is never smaller than the inverse of the condition number, and never larger than the condition number. If κ_c is too big, errors will easily “travel” along the mechanism making the control scheme more difficult and the performance worst. These ill-conditioned matrices M_c can render the control scheme useless, even in the cases where the dynamic coupling is quite big.

Example 6 This example is intended to demonstrate the different conclusions that can be drawn from the analysis of the singular values of the matrix M_c. Namely, we reexamine example 5 considering now as a measuring index the condition number of M_c. Since M_c is a 1 x 2 matrix, it has only one singular value; consequently, its condition number is always equal to 1.0, no matter where the actuators are placed.

This example demonstrates that different measures based on the same matrix can lead to different conclusions: although the condition number of M_c is constant for any positioning of the actuator, the coupling index is greater when the actuator is located closer to the base.

■

A final remark that can be made here is that the coupling index can be used in the design of the underactuated system in different ways than it was used in example 5. Namely, one may design a manipulator where some pairs of active-passive joints have maximum coupling, for easy of driving of the passive joints; at the same time, the designer may want to minimize the coupling between specific pairs of active-active, active-passive or passive-passive joints. This is reasonable, since the coupling present in manipulators is configuration-varying and highly nonlinear. At the same time the mechanism has maximum coupling between certain joints to drive the passive joints, it has minimum coupling between other joints to minimize nonlinear effects.

6 Implementation Issues

6.1 Configuration Design

After going through the analysis in section 4, one can determine the best actuator placement so as to maximize the dynamic coupling between the active and the passive joints. One may also be interested in finding out the arm configurations that yield the maximum dynamic coupling for a given design of the manipulator and its workspace. Mathematically this corresponds to finding the joint angles q that maximize the coupling index. We will illustrate this concept with an example.

Example 7 Given the underactuated manipulator in Figure 2, let's suppose an actuator is placed at joint 1. As we saw, ρ_c is this case is given by (28):

$$\rho_c = \left| 1 + \frac{m_2 l_1 l_{c_2} \cos(\theta_2)}{m_2 l_{c_2}^2 + I_2} \right|$$

The joint angle θ_2 that maximizes expression (28) can be found via:

$$\frac{d\rho_c}{d\theta_2} = -\frac{m_2 l_1 l_{c_2} \sin(\theta_2)}{m_2 l_{c_2}^2 + I_2} = 0 \qquad (48)$$

or:

$$\theta_2 = 0 \qquad (49)$$

(note that $\theta_2 = \pi$ corresponds to a point of minimum - see also Figure 3).

As we can see, the arm configuration that yields maximum dynamic coupling is the one where the arm is fully extended. Note how this differs from the results otherwise obtained when one considers the classical *manipulability measure*, introduced by Yoshikawa [12]. For a regular fully-actuated 2-DOF planar manipulator similar to the one treated in this example, this configuration yields the minimum of the manipulability measure. ■

6.2 Individual Joint Coupling

The coupling index, in addition to being useful on the design of the underactuated system, can also be used for real-time control. In [2], Bergerman and Xu demonstrated the feasibility of driving a three-link planar manipulator with only two actuators. The passive joint and one active joint (the one closest to the base) were controlled first. After the passive joint reached its set-point, it was braked, and then both active joints were controlled to their desired set-points. The active joint closer to the base was chosen to be controlled first on a rationale of reduced settling time. However, it may be the case that this joint has greater coupling with the passive joint than the other active one, so it should be used to drive the passive joint, and only be controlled after the passive joint is braked.

Basically, the idea here is to define an *individual joint coupling index* relating each passive joint to each active one. Working with these pairs of active-passive joints, we can measure the dynamic coupling existent between each of them. Ultimately, our objective will be that of determining which active joint should be chosen to drive each passive one.

Recall equation (11):

$$\ddot{q}_p = M_c \ddot{q}_a$$

If we split the expression above on its constituting lines, we have:

$$\ddot{q}_{p_i} = M_{c_{i,1}} \ddot{q}_{a_1} + \ldots + M_{c_{i,r}} \ddot{q}_{a_r} \tag{50}$$

In order to study the coupling between the *i*-th passive and the *j*-th active joint, we can assign zero values to all except the *j*-th active joint's acceleration:

$$\ddot{q}_{p_i} = M_{c_{i,j}} \ddot{q}_{a_j} \tag{51}$$

This equation resembles (11) and so we can define the *coupling index between the i-th passive and the j-th active joint*:

$$\rho_{c_{ij}} = \left| M_{c_{i,j}} \right| \tag{52}$$

For every row in the matrix M_c, the element (i, j) with greater magnitude will indicate that the greatest dynamic coupling for the passive joint i comes from the active joint j.

Example 8 We will review the example presented in [2], using the concept of individual joint coupling index defined above. The system under discussion is the one shown in Figure 7, where joints 1 and 2 are active and joint 3 is passive (according to the results in example 5). For this system, the matrix M_c was given by (41):

$$M_{c_1} = -\left[1 + 0.2727\,(c_{23} + c_3) \qquad 1 + 0.2727 c_3\right]$$

Equation (41) can also be read as:

$$\ddot{q}_{p_1} = -\,[1 + 0.2727\,(c_{23} + c_3)\,]\,\ddot{q}_{a_1} - [1 + 0.2727 c_3]\,\ddot{q}_{a_2} \tag{53}$$

According to (52) we have:

$$\begin{aligned} \rho_{c_{11}} &= \left|1 + 0.2727\,(c_{23} + c_3)\right| \\ \rho_{c_{12}} &= \left|1 + 0.2727 c_3\right| \end{aligned} \tag{54}$$

Figures 12 and 13 present the values of $\rho_{c_{11}}$ and $\rho_{c_{12}}$ for all possible combinations of θ_2 and θ_3; Figure 14 present both figures combined. Table 2 presents the maximum, minimum, average and standard deviation values for each of them.

Table 2: Maximum, minimum, average and standard deviation values attained by $\rho_{c_{11}}$ and $\rho_{c_{12}}$.

i	$\max(\rho_{c_i})$	$\min(\rho_{c_i})$	$\text{avg}(\rho_{c_i})$	$\text{std}(\rho_{c_i})$
11	1.5454	0.4546	1.0000	0.2728
12	1.2727	0.7273	1.0000	0.1929

For this system it is difficult to tell which active joint has greater coupling with the passive one. Although $\rho_{c_{11}}$ attains greater values than $\rho_{c_{12}}$, it also attains smaller values; and the averages of both indexes are the same. This example shows that the coupling index, although useful, may not provide the control engineer with sufficient information to decide on which active joint should drive the passive one. Global indexes, based on the integral of the coupling index, may be more useful in this case, as it will be shown in the sequence. ■

6.3 Global Coupling Index

The coupling index defined previously is a local measure; it measures the “amount” of dynamic coupling between the active and the passive joints at every point in the joint space. The greater the coupling index at a particular configuration of the manipulator, the easier for the active joints to drive the passive ones.

However, in design and path planning problems, one is more interested in the coupling index in a global sense, so as to measure the dynamic coupling existent within the workspace of the manipulator. In this case, a *global coupling index* is more useful, for it will measure the coupling between the joints at *all* points in the joint space.

One possible way of defining a global coupling index is as follows [4]:

$$\rho_c^g = \frac{\int_\Theta \rho_c^2 d\Theta}{\int_\Theta d\Theta} \tag{55}$$

where the integrals above are taken over the entire joint space $\Theta \in \Re^n$ of the manipulator. The use of the squared value of the coupling index is inert because the coupling index is always non-negative; and this choice facilitates the problem of finding a closed-form solution to the above integral, because the singular values of a matrix A are equal to the positive square roots of the nonzero eigenvalues of $A^T A$.

This choice of the global coupling index will take into account not only the local coupling between the joints, but that available over the entire joint space, as the next examples show.

Example 9 We re-analyze now example 5, where the objective was to determine the best actuator placement based on the dynamic coupling between the joints. There, the decision to place the actuators on joints 1 and 2 was based on the maximum, minimum and average values of ρ_c for the various possible configurations. Here we can base this decision on a global index, which already takes into account all these quantities.

For a 1 x 2 matrix, the unique singular value is computed easily as:

$$A = \begin{bmatrix} a_1 & a_2 \end{bmatrix} \Rightarrow \sigma = \sqrt{a_1^2 + a_2^2} \tag{56}$$

Consequently, comparing A above with the various M_{c_i}, $i = 1, 2, 3$, of example 5, we have:

$$\rho_{c_i}^{g} = \frac{\int_{\Theta}\left(a_1^2 + a_2^2 \right) d\Theta}{\int_{\Theta} d\Theta} \tag{57}$$

We considered in the following calculations that the joints can rotate freely around their respective axis from 0 to 2π. In cases where there are physical joint limits, this can be taken into account in the calculation of the integrals in (55). For cases 1, 2, and 3 studied in example 5, we have the results shown in table 3.

Table 3: Global coupling index $\rho_{c_i}^{g}$, $i = 1, 2, 3$.

i	$\rho_{c_i}^{g}$
1	2.1115
2	1.2041
3	0.2090

We can immediately conclude that case 1 is the one which provides greater dynamic coupling between the active and the passive joints in a global sense. Note that this is the same conclusion as the one drawn in example 5, reached in a much simpler way. ■

Example 10 The global coupling index can also be used in conjunction with the individual joint coupling index defined in section 6.2. The idea is to use the later instead of ρ_c in equation (55):

$$\rho_{c_{ij}}^{g} = \frac{\int_{\Theta} \rho_{c_{ij}}^2 \, d\Theta}{\int_{\Theta} d\Theta} \tag{58}$$

Calculating the above *global individual joint coupling index* for the manipulator in example 8, we have the results shown in table 4.

As the result shows, the global coupling between the first and second active joints and the passive joint is exactly the same. For control purposes, then, one can choose either active joint to dynamically control the passive joint.

Table 4: Global individual joint coupling indexes $\rho^g_{c_{11}}$ and $\rho^g_{c_{12}}$.

i	$\rho^g_{c_i}$
11	1.0372
12	1.0372

Note again that this conclusion was drawn immediately, as opposed to example 8, where no conclusion could be drawn. ■

Example 11 The coupling index can also be useful for the purpose of designing the links of an underactuated mechanism. Suppose in the manipulator of Figure 2, with joint 1 active, we have available the following parameters: $m_2 = 1\text{Kg}$, $I_2 = 0.1\text{Kg}\cdot\text{m}^2$, $l_1 = 1\text{m}$. Additionally, suppose we want to determine l_{c_2} so as to maximize the global coupling index ρ^g_c. In this case we have:

$$\rho_c = \left| 1 + \frac{l_{c_2}\cos(\theta_2)}{0.1 + l^2_{c_2}} \right| \tag{59}$$

$$\rho^g_c = \frac{1 + 70l^2_{c_2} + 100l^4_{c_2}}{1 + 20l^2_{c_2} + 100l^4_{c_2}} \tag{60}$$

Figure 15 presents the global coupling index as a function of l_{c_2}. As we can see, for $l_{c_2} = 0.316\text{m}$, it attains the maximum value $\rho^g_c = 2.250$. This example shows how the global coupling index can be used for design issues other than actuator placement.

7 Conclusion

There has been considerable progress recently in the area of analysis and control of underactuated manipulators. The current literature in this area however, has always assumed that sufficient dynamic coupling was available between the active and passive joints for effective control of the manipulator. Because this assumption is not always valid, it is vital for design, analysis, and control of these systems that the amount of available coupling be quantified.

In this work, the authors have proposed a measure of the dynamic coupling between the active and passive joints of an underactuated manipulator. The coupling index indicates precisely the amount of coupling available for the purpose of controlling the passive joints of the manipulator through the application of torques in the active joints. We have also proposed a global coupling index, which indicates the amount of coupling available over the entire workspace of the manipulator.

As we have shown through a series of illustrative examples, the proposed indices can be used effectively within the contexts of mechanical design, configuration optimization, and real-time control. Moreover, when redundant degrees of freedom are available in an underactuated manipulator, these indices may be used as local measures for use within a redundant control scheme.

8 Acknowledgments

We would like to acknowledge the fruitful discussion with Christiaan Paredis, Carnegie Mellon University, regarding the issue of positive-definiteness of the new inertia matrix. The first author is supported by a grant from the Brazilian National Council for Research and Development (CNPq).

9 References

[1] Arai, H.; Tachi, S. Position control of a manipulator with passive joints using dynamic coupling. *IEEE Transactions on Robotics and Automation*, vol. 7, no. 4, Aug. 1991, pp. 528-534.

[2] Bergerman, M.; Xu, Y. Robust control of underactuated manipulators: analysis and implementation. *Proceedings of the IEEE Systems, Man and Cybernetics Conference*, Oct. 1994.

[3] Craig, J.J. *Introduction to robotics*: Mechanics and control. Addison-Wesley, Reading, 2 ed., 1989.

[4] Gosselin, C.; Angeles, J. A global performance index for the kinematic optimization of robotic manipulators. *Transactions of the ASME, Journal of Mechanical Design*, vol. 113, Sep. 1991, pp. 220-226.

[5] Lancaster, P.; Tismenetsky, M. *The theory of matrices*. Academic Press, Orlando, 2 ed., 1985.

[6] Lee, C.; Xu. Y. *Actuability of underactuated manipulators*. CMU-TR-RI-94-13, Carnegie Mellon University, May 1994.

[7] Mukherjee, R.; Chen, D. Control of free-flying underactuated space manipulators to equilibrium manifolds. *IEEE Transactions on Robotics and Automation*, vol. 9, no. 5, Oct. 1993.

[8] Nakamura, Y. *Advanced robotics*: Redundancy and optimization. Addison-Wesley, Reading, 1ed., 1991.

[9] Oriolo, G.; Nakamura, Y. Control of mechanical manipulators with second-order nonholonomic constraints: underactuated manipulators. *Proceedings of the 30th Conference on Decision and Control*, Dec. 1991, pp. 2398-2403.

[10] Papadopoulos, E.; Dubowsky, S. Failure recovery control for space robotic systems. *Proceedings of the 1991 American Control Conference*, vol. 2, 1991, pp. 1485-1490.

[11] Xu, Y; Shum, H. Y. Dynamic control and coupling of free-floating space robot systems. (To appear in *Journal of Robotic Systems).*

[12] Yoshikawa, T. *Foundations of robotics*: Analysis and control. MIT Press, Cambridge, 1ed., 1990.

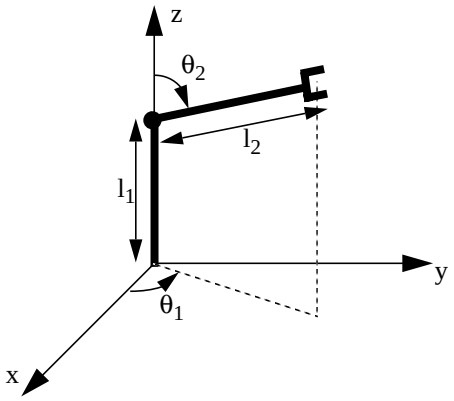

Figure 1: Two-link manipulator with rotary joints.

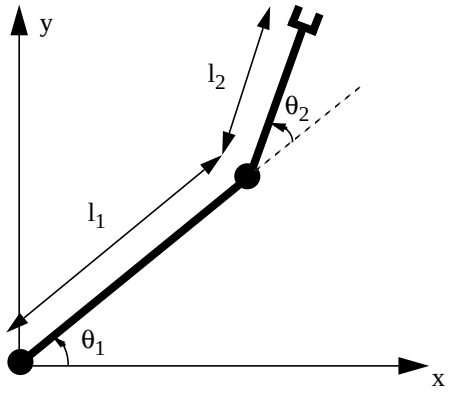

Figure 2: Two-link planar manipulator with rotary joints.

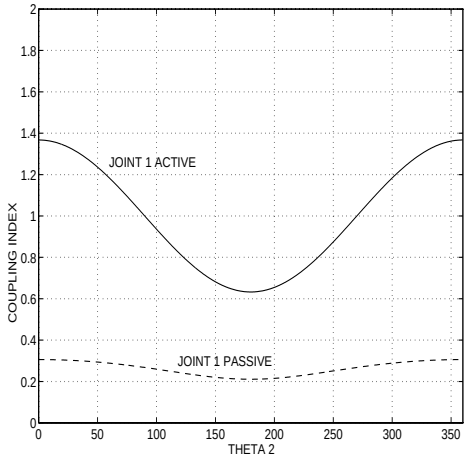

Figure 3: Coupling index between the joints of the robot in Figure 2.

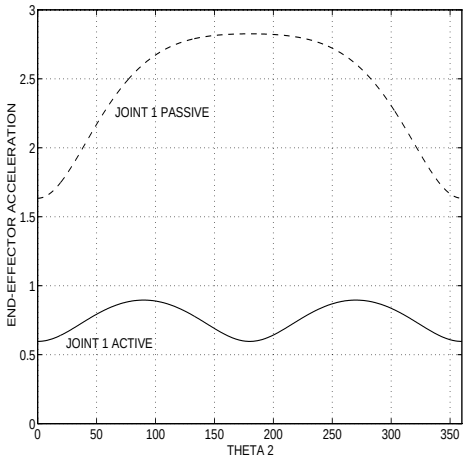

Figure 4: End-effector acceleration for the mechanism in Figure 2.

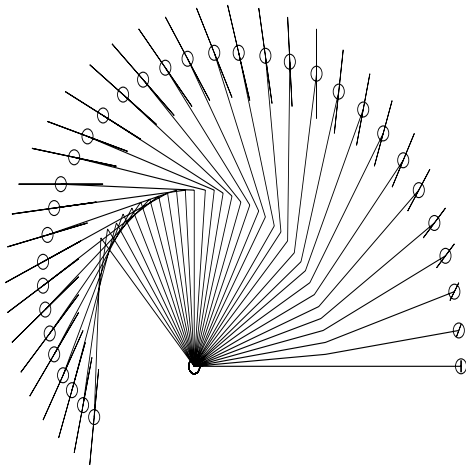

Figure 5: Actuability index for the lower-actuated mechanism in Figure 2.

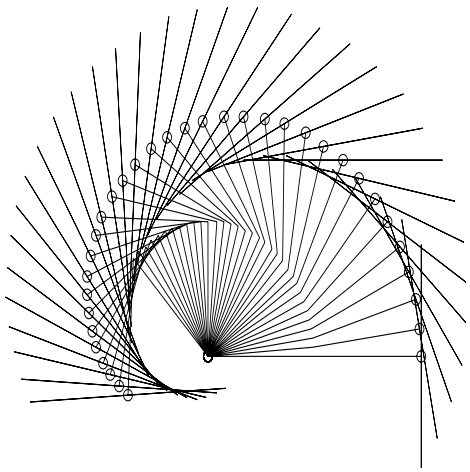

Figure 6: Actuability index for the upper-actuated mechanism in Figure 2.

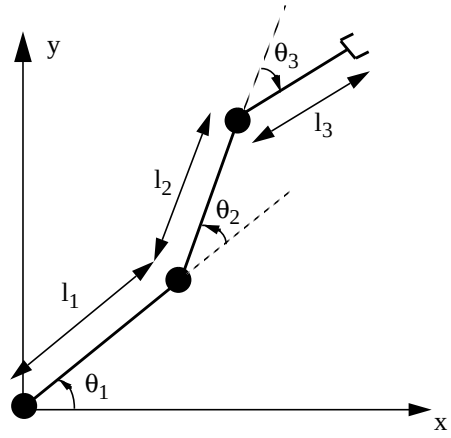

Figure 7: Three-link planar manipulator with rotary joints.

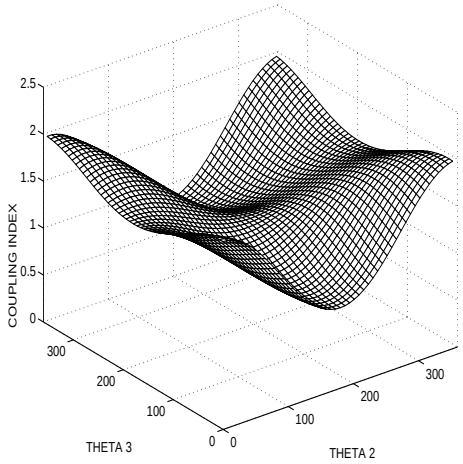

Figure 8: Coupling index for the manipulator in Figure 7, when joint 3 is passive.

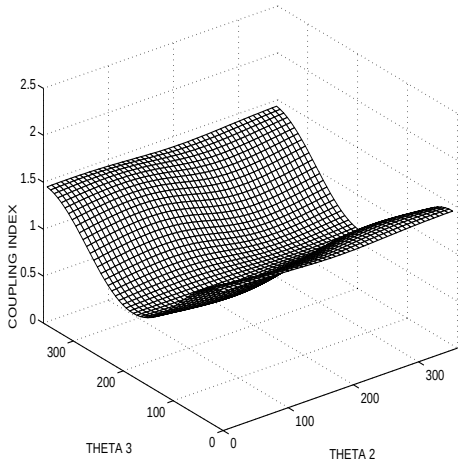

Figure 9: Coupling index for the manipulator in Figure 7, when joint 2 is passive.

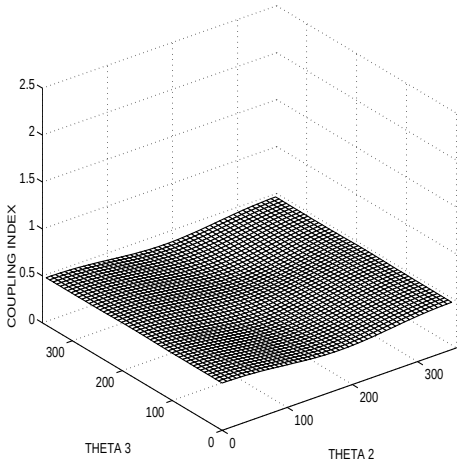

Figure 10: Coupling index for the manipulator in Figure 7, when joint 1 is passive.

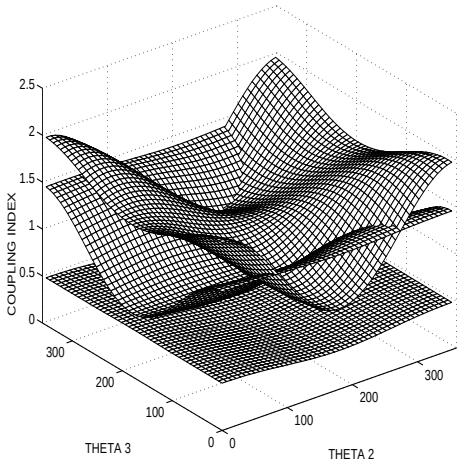

Figure 11: Coupling indexes for the manipulator in Figure 7.

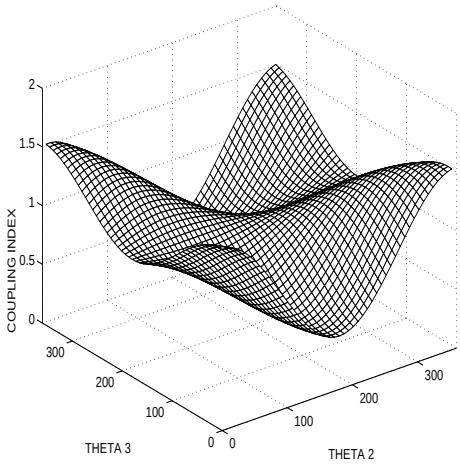

Figure 12: Individual coupling index between joints 1 and 3 of the manipulator in Figure 7.

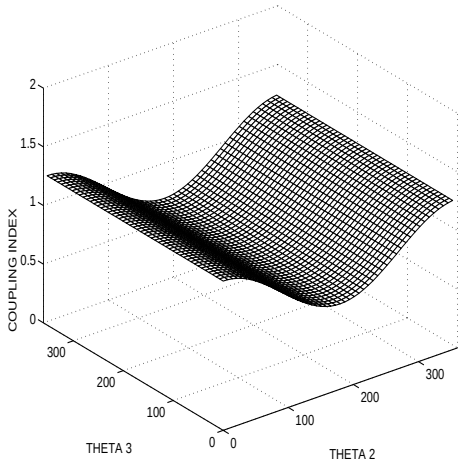

Figure 13: Individual coupling index between joints 2 and 3 of the manipulator in Figure 7.

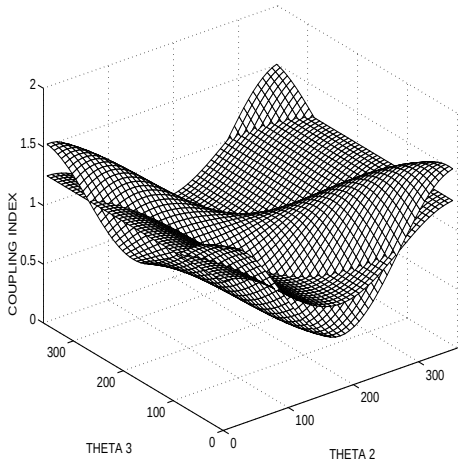

Figure 14: Individual coupling indexes for the manipulator in Figure 7.

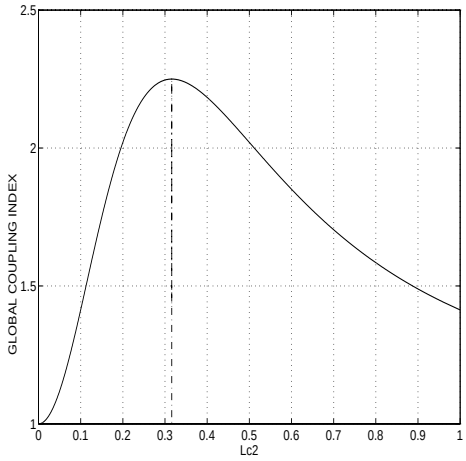

Figure 15: Global coupling index in example 11.